

## Ribonuclease like 5 regulates zebrafish yolk extension by suppressing a p53-dependent DNA damage response pathway



Yixing Zhai<sup>a,c,d</sup>, Xinyuan Zhao<sup>a,c,d</sup>, Jinghao Sheng<sup>a,c,d</sup>, Xiangwei Gao<sup>a,c,d</sup>, Zhao Ou<sup>e</sup>, Zhengping Xu<sup>a,b,c,d,\*</sup>

<sup>a</sup> Institute of Environmental Health, Zhejiang University School of Public Health, Hangzhou 310058, China

<sup>b</sup> Collaborative Innovation Center for Diagnosis and Treatment of Infectious Diseases, Zhejiang University, Hangzhou 310003, China

<sup>c</sup> Program in Molecular Cell Biology, Zhejiang University School of Medicine, Hangzhou 310058, China

<sup>d</sup> Research Center of Molecular Medicine, Zhejiang University School of Medicine, Hangzhou 310058, China

<sup>e</sup> Key Laboratory for Molecular Animal Nutrition, Ministry of Education, Zhejiang University College of Animal Sciences, Hangzhou 310058, China

### ARTICLE INFO

#### Article history:

Received 9 December 2014

Received in revised form 10 April 2015

Accepted 5 May 2015

Available online 14 May 2015

#### Keywords:

Ribonuclease like 5

Yolk extension

P53

DNA damage

Embryogenesis

### ABSTRACT

*Ribonuclease like 5 (Rnasel5)* is a novel member of the zebrafish ribonuclease A family and its expression is increased during early embryogenesis. However, the *in vivo* biological function of *Rnasel5* remains to be elucidated. Here, we report that knockdown of *Rnasel5* by morpholinos caused shrunken yolk extension as well as increased DNA damage at yolk syncytial layer and external tissue layers via the activation of p53 pathway. In addition, the morphological defects caused by *Rnasel5* knockdown can be partially rescued by mRNA injection. Our findings provide the first functional characterization of *Rnasel5* in zebrafish development and reveal its critical role in yolk extension by modulation of the p53 pathway.

© 2015 Elsevier Ltd. All rights reserved.

## 1. Introduction

The secreted and vertebrate specific ribonuclease A (RNASE A) family comprises a large group of structurally similar proteins that catalyze the degradation of RNA into smaller fragments. Members of this family share sequence homology of specific elements, adapt a unique disulfide-bonded tertiary conformation, and display an array of biological activities ranging from cytotoxicity to angiogenesis. To date, five zebrafish RNASE members, named as *ribonuclease like 1, 2, 3, 4, and 5*, respectively, have been identified (Pizzo et al., 2006, 2011). Although the expression patterns, protein structures and *in vitro* functions of them have been studied, *in vivo* functional characterization of this family is lacking (Kazakou et al., 2008; Monti et al., 2009; Pizzo et al., 2011; Quarto et al., 2008). *Ribonuclease like 5 (Rnasel5)* is a novel member of the zebrafish RNase A family that was first identified and characterized by Pizzo et al. (2011). It has been revealed that *Rnasel5* possesses

low ribonucleolytic activity, while its angiogenic capacity is similar to human angiogenin/ribonuclease-5 (Pizzo et al., 2011). However, little is known about the physiological role of *Rnasel5* in vertebrate development. Given that zebrafish is an excellent model for the study of development, we adopted this model system to investigate whether *Rnasel5* plays a role in zebrafish embryogenesis.

Yolk extension consists of an internal yolk cell with an outer cortical layer including yolk syncytial layer (YSL), a sheath of cellular mesendodermal mantle and external embryonic integument consisting of an embryonic epidermis plus enveloping layer (EVL), and exists as a cylindrical mass elongated from the spherical yolk ball (Virta and Cooper, 2011). The yolk extension becomes detectable at the segmentation period and progresses from 16 hpf (hours post fertilization) to 24 hpf in zebrafish (Virta and Cooper, 2011). It performs several functions in early development such as nutrient transport (Lyman Gingerich et al., 2006), utilization of maternally stored morphogenetic substances including retinoids (Isken et al., 2007), and morphogenesis (Mizuno et al., 1999; Ober and Schulte-Merker, 1999). However, little is known about the factors that regulate yolk extension development. Recently, it has been reported that knockdown of Rbp4 (retinol binding protein 4) in the YSL resulted in shortened yolk extension (Li et al., 2007). Depletion of Rpl11 (ribosomal protein L11), a regulator of p53 activity,

\* Corresponding author at: Institute of Environmental Health, Zhejiang University School of Public Health, 866 Yuhangtang Road, Hangzhou 310058, China.  
Tel.: +86 571 88208008; fax: +86 571 88208164.

E-mail address: [zpxu@zju.edu.cn](mailto:zpxu@zju.edu.cn) (Z. Xu).

induces yolk extension defects and massive apoptosis especially in the primary head region (Chakraborty et al., 2009). Here, we report a new yolk extension regulator *Rnasel5* and its mechanism of action underlying its activity.

## 2. Materials and methods

### 2.1. Fish lines

Zebrafish fish lines (wild type AB line and *tp53<sup>M214K</sup>*) were maintained in the fish facility at the Key Laboratory for Molecular Animal Nutrition, Ministry of Education, Zhejiang University College of Animal Sciences and in compliance with Institute Animal Care and Use Committee (IACUC).

### 2.2. RNA isolation and quantitative real-time PCR (RT-qPCR)

Total RNA was extracted from embryos using TRIzol reagent (Invitrogen). Then reverse transcription was performed by Superscript II reverse transcription kit (Invitrogen). Then, the quantitative real-time PCR were performed with specific primers listed in Table 1. The PCR products were confirmed by DNA sequencing.

### 2.3. Whole-mount mRNA in situ hybridization (WISH)

To visualize the expression pattern of *Rnasel5*, we used digoxigenin (DIG)-labeled full-length *Rnasel5* mRNA as probe to carry out WISH analysis. Embryos were fixed in 4% paraformaldehyde (PFA), hybridized with the DIG-labeled RNA probe in hybridization buffer at 68 °C, and then incubated with anti-DIG antibody conjugated with alkaline phosphatase (AP). After staining with Nitroblue Tetrazolium/5-Bromo-4-chloro-3-Indolyl Phosphate (NBT/BCIP) substrate solution, the embryos were observed with VH-M100 Microscopy System. To do WISH on cryosections, we first fixed the embryos in 4% PFA and cryosectioned them after embedded with low-melting agarose gel and optimum cutting temperature compound. The slides were hybridized as described above.

### 2.4. Morpholino oligonucleotides (MOs) and mRNA injections

Two *Rnasel5* antisense MOs were designed and used in the present study: MO-1: 5'-CGGCAGACTGAAGAATCTCCATGAC-3', which specifically targets ATG region of *Rnasel5*; MO-2: 5'-TTGTAAGTGAACCCAACCTTGCTT-3', which targets the 5'UTR of *Rnasel5*. The sequence of the standard control MO is 5'-CCTCTTACCTCAGTTACAATTATA-3'. p53 MO sequence (5'-GGCCATTGCTTGCAAGAATTG-3') was adopted as previously described that targets the p53 ATG region (Robu et al., 2007). MOs were resuspended in DEPC water at a concentration of 5 nM as stock solutions. For microinjection into embryos, a 0.5 nl volume of each 1.0 mM MO-1, 2.0 mM MO-2, 0.8 mM p53 MO or 1.0 mM Ctrl MO solution was injected into the yolk during the one-cell

stage of embryos. For the rescue experiment, MO resistant full-length *Rnasel5* mRNA was co-injected with MO at a concentration of 200 pg/embryo.

### 2.5. TUNEL assay

For detection of DNA damage in the yolk extension region, a TUNEL assay was performed on the cryosections using an *in situ* Cell Death Detection kit (Roche) according to the manufacturer's instructions. TUNEL and immunofluorescence double assay was performed the immunofluorescence firstly using the monoclonal antibody against zebrafish Betaine homocysteine S-methyltransferase (Bhmt) as the primary antibody followed by an Alexa Fluor 488-labeled (Invitrogen) secondary antibody (Yang et al., 2011). Then the same specimens were subjected to the TUNEL assay. The images were taken by Nikon A1 confocal microscope.

### 2.6. Quantitative analysis and statistics

Data processing and statistical analyses were performed using Prism Graph version 6.0. This software was used to generate each of the graphs shown in the text to perform statistical tests where appropriate. The ImageJ version 1.48 was used to measure the yolk area and count the TUNEL positive cells. Data are expressed as means ± S.D. from three independent experiments. Differences were declared significant at \*:  $P < 0.05$  and \*\*:  $P < 0.01$ .

## 3. Results

### 3.1. Temporal and spatial expression patterns of *Rnasel5* during early embryonic development in zebrafish

The three-dimensional structure, physicochemical properties, and biological properties of *Rnasel5* have been identified and characterized (Pizzo et al., 2011). However, the temporal and spatial expression of *Rnasel5* remains to be clarified. Therefore, we first determined the temporal expression of *Rnasel5* mRNA during early zebrafish embryonic development by RT-qPCR (Fig. 1A). The data revealed that zygotic transcription of *Rnasel5* was activated at gastrula period (6 hpf), and the amount of transcripts increased throughout the period of somitogenesis (10–24 hpf). Then, we further analyzed its spatial expression by WISH (Fig. 1B). A faint staining was visible in the embryos before the gastrula stage. The *Rnasel5* transcripts localized within the anterior-posterior embryonic axis and the ventral of the trunk. Interestingly, the expression of *Rnasel5* was also detected in layers around the yolk ball and yolk extension, indicating this protein may involve in the formation or maintenance of yolk extension. Moreover, *in situ* hybridization on cryosections of 24 hpf embryos further confirmed the expression of *Rnasel5* in the overlying layers of yolk cell (Fig. 1C).

### 3.2. *Rnasel5* depletion results in severe morphological defects

To investigate the function of *Rnasel5* in early embryogenesis, we used two distinct morpholinos (MO-1 and MO-2) to inhibit its translation in zebrafish embryos. The lowest effective concentration of MOs was determined by titration with mortality and morphological examination (Fig. 2A and B). Accordingly, we determined 0.5 pmol/embryo for MO-1 and 1.0 pmol/embryo for MO-2 as an optimal dose (15% mortality) and used this dose throughout our study. The efficiency of the MOs was verified by co-injection of MOs and EGFP-tag reporters containing the target region of MOs, followed by observation of the GFP signal intensity. We found that, compared to the control group, GFPs in embryos with *Rnasel5* MOs were decreased, demonstrating an efficient inhibition of *Rnasel5* by each individual MO (Fig. 2C).

**Table 1**  
Primers used in this work.

No.	Primer name	Sequence (5'-3')
1	<i>Rnasel5</i> -Fw	AAGGTTCACCAGACGTAGAT
2	<i>Rnasel5</i> -Rv	TATTTAGCTGACCTGTTAC
3	<i>odc1</i> -Fw	TTGAATCAAATCTGAACAAA
4	<i>odc1</i> -Rv	GGAGGTGCTCTTCAGGACA
5	<i>p21</i> -Fw	GAAGCCAAACAGACCAACAT
6	<i>p21</i> -Rv	GCAGCTCAATTACGATAAAGA
7	<i>Bax</i> -Fw	GGAGCCGATACGGGACTG
8	<i>Bax</i> -Rv	TTGCCAATCACCAATGCTGTG
9	<i>tp53</i> -Fw	TGGAGAGGAGGTGGCAAATCAA
10	<i>tp53</i> -Rv	GACTGGGGAACCTGAGCCTAAAT

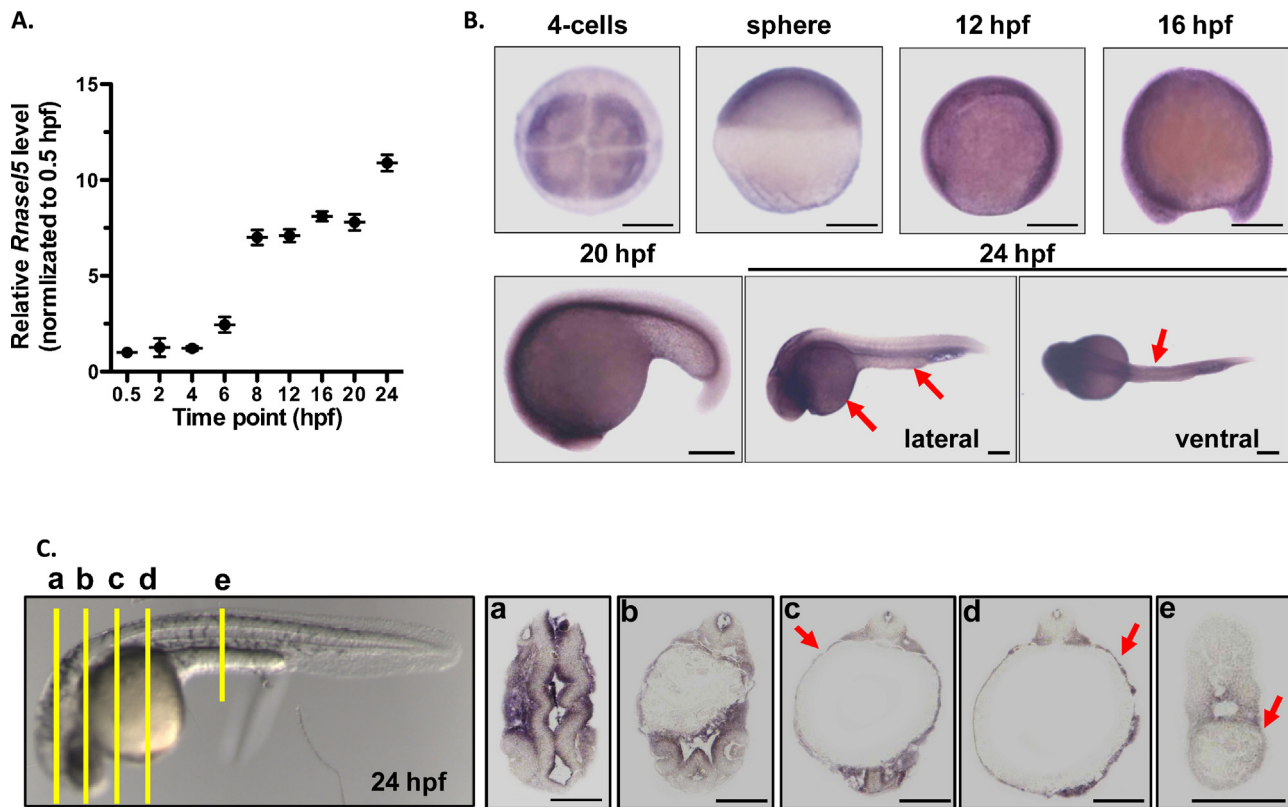


**Fig. 1.** Temporal and spatial expression patterns of *Rnasel5* during early embryonic development in zebrafish. (A) RT-qPCR assay was performed to detect *Rnasel5* expression level from 0.5 hpf to 24 hpf. (B) Spatial expression patterns of *Rnasel5* at different stages were detected by WISH. The red arrows show *Rnasel5* located on the anterior-posterior embryonic axis and the ventral of the trunk at 24 hpf, scale bar 100  $\mu$ m. (C) Cross sections of WISH in left panel embryo as indicated by yellow line. Red arrow indicates *Rnasel5* located in the overlying layers of yolk, scale bar 100  $\mu$ m. (For interpretation of the references to color in this figure legend, the reader is referred to the web version of the article.)

Monitoring the embryos treated with different morpholinos at early time points revealed a defect in hatching in *Rnasel5* morphants. For example, at 2.5 dpf, 97% of embryos treated with control MO hatched, while only 1.7% of MO-1-treated and 4.3% of MO-2-treated ones hatched (Fig. 2D). The failure of hatching or delay to hatch resulted in a decreased survival at a later time point. Compared to the control MO injected embryos that showed a >80% (42/53) survival at 5 dpf, only <34% (22/64) of MO-1 and <50% (27/54) MO-2 embryos survived (Fig. 2E). More severely, the *Rnasel5* MOs-injected embryos could hardly survive to the time point of 7 dpf, suggesting that *Rnasel5* knockdown is embryonic lethal. Significantly, the defects in development caused by *Rnasel5* knockdown can be, at least partially, rescued by a co-injection of the *Rnasel5* mRNA (Fig. 2D and E). As the human homolog of *Rnasel5* is related to angiogenesis (Gao and Xu, 2008; Pizzo et al., 2011; Sheng et al., 2014), we continued to examine the effect of *Rnasel5* on angiogenesis in transgenic zebrafish line Tg(*fli1*:EGFP)<sup>y1</sup>, which expresses enhanced GFP in the entire vasculature under the control of the *fli1* promoter. Our results showed that most of the intersegmental vessels (ISVs) failed to sprout from the dorsal aorta (DA) at 24 hpf in *Rnasel5* morphants, while ISVs had sprouted already and extended above the horizontal myoseptum at the same time point in control embryos, indicating *Rnasel5* plays an important role in zebrafish angiogenesis (Fig. 2F).

### 3.3. Knockdown of *Rnasel5* causes severe yolk extension defects

Interestingly, we found that the major defects in *Rnasel5* morphants were in the yolk extension region. Yolk extension development starts from 14-somite stage at 16 hpf and extends to primary larvae at 24 hpf. The yolk extension showed slightly

difference between control group and *Rnasel5* morphants at the middle stage of somitegenesis (20 hpf) (Fig. 3A, left panel). However, severe yolk extension defects, even complete disappearance of yolk extension, were observed in *Rnasel5* morphants at 24 hpf (Fig. 3A, right panel). To confirm our observation, hematoxylin and eosin staining (H&E staining) on cryosections of the 24 hpf embryos were performed. As shown in Fig. 3B, the cross-sectional area of yolk extension was reduced in *Rnasel5* morphants. The yolk extension defects can be partially rescued by co-injecting *Rnasel5* mRNA. Quantitative analyses of these phenotypes were also carried out and shown in Fig. 3C and D. These results indicated that the maintenance of yolk extension was severely affected by the depletion of *Rnasel5*.

### 3.4. Yolk extension defect of *Rnasel5* morphant results from increased DNA damage in the YSL and external tissue layers

The formation and maintenance of yolk extension correlates with the yolk syncytial layer and external tissue layers including the mesendodermal mantle, the embryonic epidermis, and the EVL (Lyman Gingerich et al., 2006). It is possible that the changes in the overlying layers of yolk are associated with yolk extension defect. In addition, angiogenin/Rnase5 (RNASE5), the human homologous gene of *Rnasel5*, has been shown to regulate cellular apoptosis (Li et al., 2010; Sadagopan et al., 2012). Therefore, we carried out TUNEL assay on the cryosections of *Rnasel5* morphants, mRNA rescue group and control group at 24 hpf. Almost no TUNEL positive nuclei was detected in the control group; however, significant amount of TUNEL-positive nuclei was observed in the overlying layers of the yolk from *Rnasel5* morphants, while decreased again in mRNA-rescue group (Fig. 4A–D). To reveal which layer did the

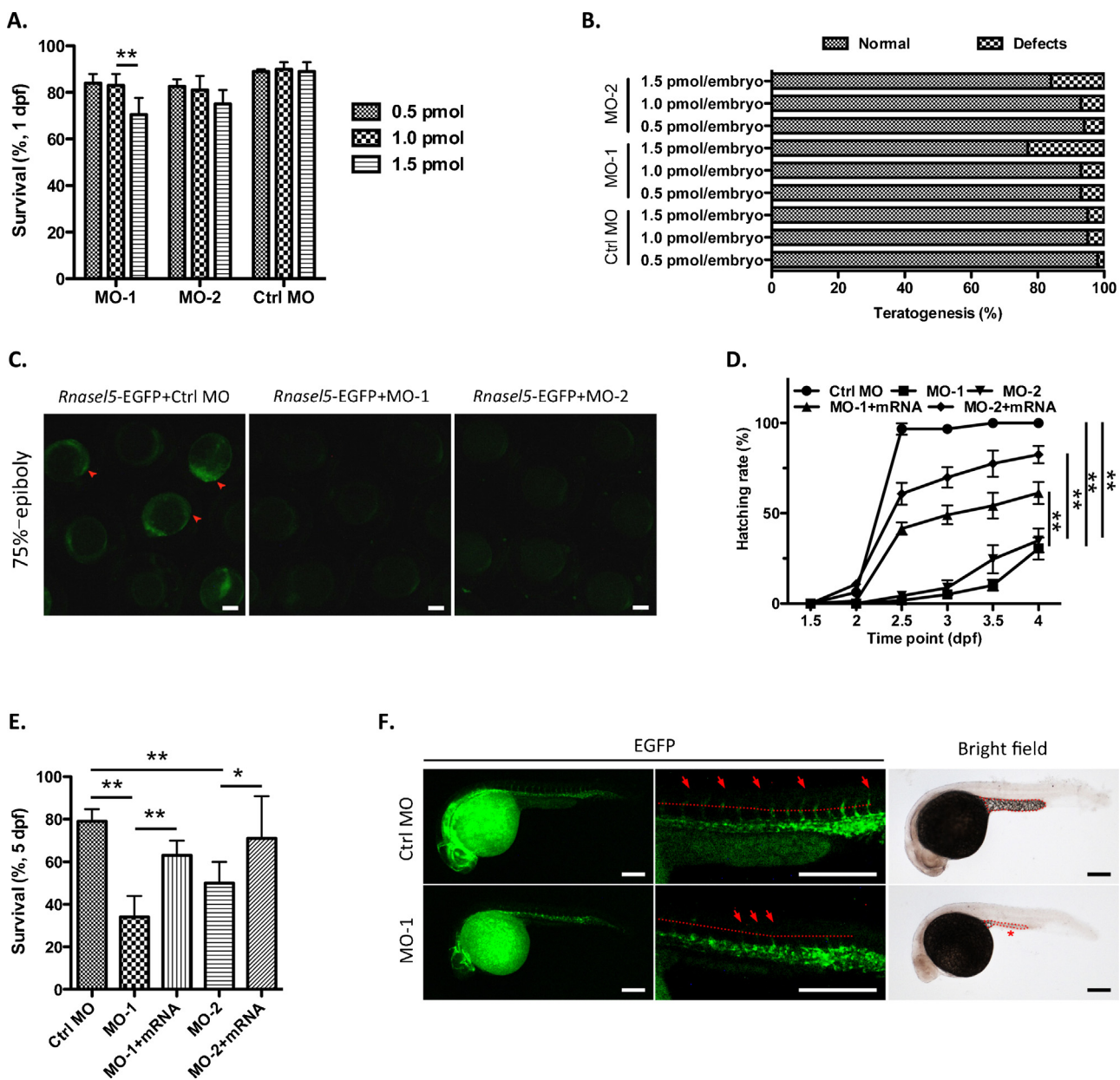


**Fig. 2.** The effects of *Rnasel5* depletion on zebrafish. (A and B) Optimization of *Rnasel5* MO's concentration. The survival rates (A) and teratogenesis (B) of embryos were analyzed after treating with different concentration of MOs at 1 dpf. (C) The efficiencies of *Rnasel5* MOs. The GFP expression level of EGFP-tag reporter was decreased after co-injecting with MOs, scale bar 100  $\mu$ m. (D) Hatching time and rates of embryos under different treatment. (E) The survival rates of embryos treated with MOs at 5 dpf. (F) The effect of *Rnasel5* on sprouting of intersegmental vessels (ISVs) in *Tg(fli1:EGFP)*<sup>y1</sup>. Embryos injected *Rnasel5* MO-1 and control MO were observed under fluorescence microscope. The red arrow shows the ISVs of zebrafish. The red dotted line shows the horizontal myoseptum of zebrafish, scale bar 100  $\mu$ m. \*:  $P < 0.05$ , \*\*:  $P < 0.01$ . (For interpretation of the references to color in this figure legend, the reader is referred to the web version of the article.)

DNA damage occur, we performed *Bnmt* staining (a YSL marker in early embryogenesis (Yang et al., 2011)) in the TUNEL assay slides, and found that the DNA damage was identified in the nuclei of yolk syncytial layer, as well as external tissue layers (Fig. 4E and F). Taken together, these data indicated that *Rnasel5* knockdown induced DNA damage in the overlying layers of yolk, especially YSL, which eventually resulted in yolk extension defects.

### 3.5. p53 pathway is activated in *Rnasel5* morphants and is associated with yolk extension defects

Several reports have pointed out that p53 pathway may be associated with the yolk extension defects, and this pathway is also important in the response to DNA damage (Chakraborty et al., 2009;

Chen et al., 2006, 2009). Actually, p53 protein was prominently up-regulated in *Rnasel5* morphants at 24 hpf, compared the control and mRNA-rescue group (Fig. 5A). Two p53 downstream targets, *p21* and *Bax*, were significantly elevated at the RNA level in *Rnasel5* morphants, indicating knockdown of *Rnasel5* results in triggered activation of p53 pathway (Fig. 5B).

To determine whether activation of p53 mediates the yolk extension defects in *Rnasel5* morphants, we injected p53 specific MO into the *Rnasel5* morphants to inhibit the translation of p53. As shown in Fig. 5C–E, the yolk extension defects in *Rnasel5* morphants were partially rescued by p53 MO. In addition, the hatching rate and survival rate were also increased in the p53 and *Rnasel5* MOs co-injected fishes compared to those in *Rnasel5* morphants (data not shown). To further confirm the role of p53 in the *Rnasel5*

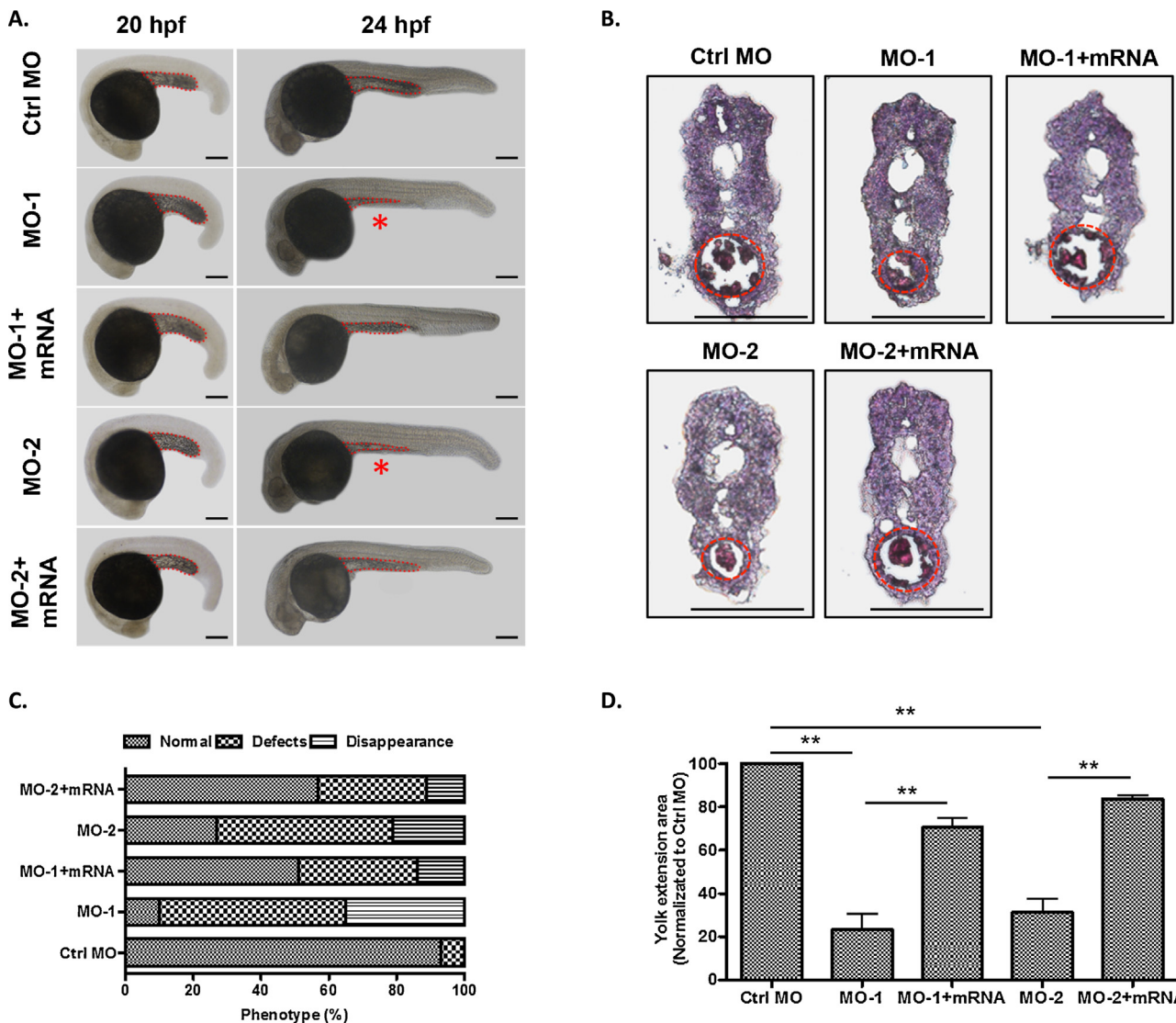


**Fig. 3.** *Rnasel5* depletion results in severe yolk extension defects. (A) MOs injected embryos were photographed at 20 hpf and 24 hpf. The shrunken yolk extension was identified with asterisk, scale bar = 100 μm. (B) H&E staining was performed on cryosections of the 24 hpf embryos. The yolk extension region was shaped by dotted red line, scale bar 100 μm. (C) Quantitative analysis data of different morphological phenotype (including normal, defects, and disappearance of yolk extension) in morphants. (D) The relative yolk extension region area of different morphants as indicated. All differences are significant, \*\*: P<0.01. (For interpretation of the references to color in this figure legend, the reader is referred to the web version of the article.)

depletion-caused yolk extension defects, we introduced a fish line with transgenic *tp53<sup>M214K</sup>*, a mutant on p53 DNA-binding domain to block the activation of p53. As expected, knockdown of *Rnasel5* did not cause the yolk extension defects in these transgenic fishes (Fig. 5F–H). These results indicated that yolk extension defects in *Rnasel5* morphants is mediated by the p53 pathway.

#### 4. Discussion

To date, five members of the RNASE A family have been identified in zebrafish; however, their functions *in vivo* are less understood. In the present study, we characterized, for the first time, the developmental effects of *Rnasel5*, a newly identified member of the zebrafish RNASE A family. We found that *Rnasel5* is a novel regulator of yolk extension development as well as an inducer of DNA damage in the overlying layers of yolk extension. Specifically, knockdown of *Rnasel5* induced defects in yolk extension and apoptosis via activation of the p53 pathway. In addition, similar to human RNASE5/angiogenin, *Rnasel5* was also involved in

vascular development (Fig. 2F). Certainly, the underlying mechanisms and relationship between different phenotypes need to be further elucidated.

The three structural components of the yolk extension interact with each other in a hierarchical manner to help elongate the cylindrical yolk extension formation (Lyman Gingerich et al., 2006; Virta and Cooper, 2011). Here, we showed that DNA damage caused by *Rnasel5* deficiency in the overlying layers of yolk extension resulted in shrunken or even disappearance of yolk extension. Several genes have been reported to regulate the yolk extension formation. For example, the *Kugelig* (*Kgg*) and *Homeobox A13a* (*HoxA13a*) are necessary for the development of yolk extension (Crow et al., 2009; Davidson et al., 2003). It would thus be interesting to investigate the cross-talk and temporal expression of these genes on the development of yolk extension. Moreover, yolk extension defects induced by *Rnasel5* deficiency occurred at the latter stage of yolk extension formation (20–24 hpf). We therefore propose that *Rnasel5* may maintain the integrity of yolk extension. Overall, our study reveals that the temporal and spatial expression pattern of *Rnasel5* is important for the proper development of yolk extension. Of

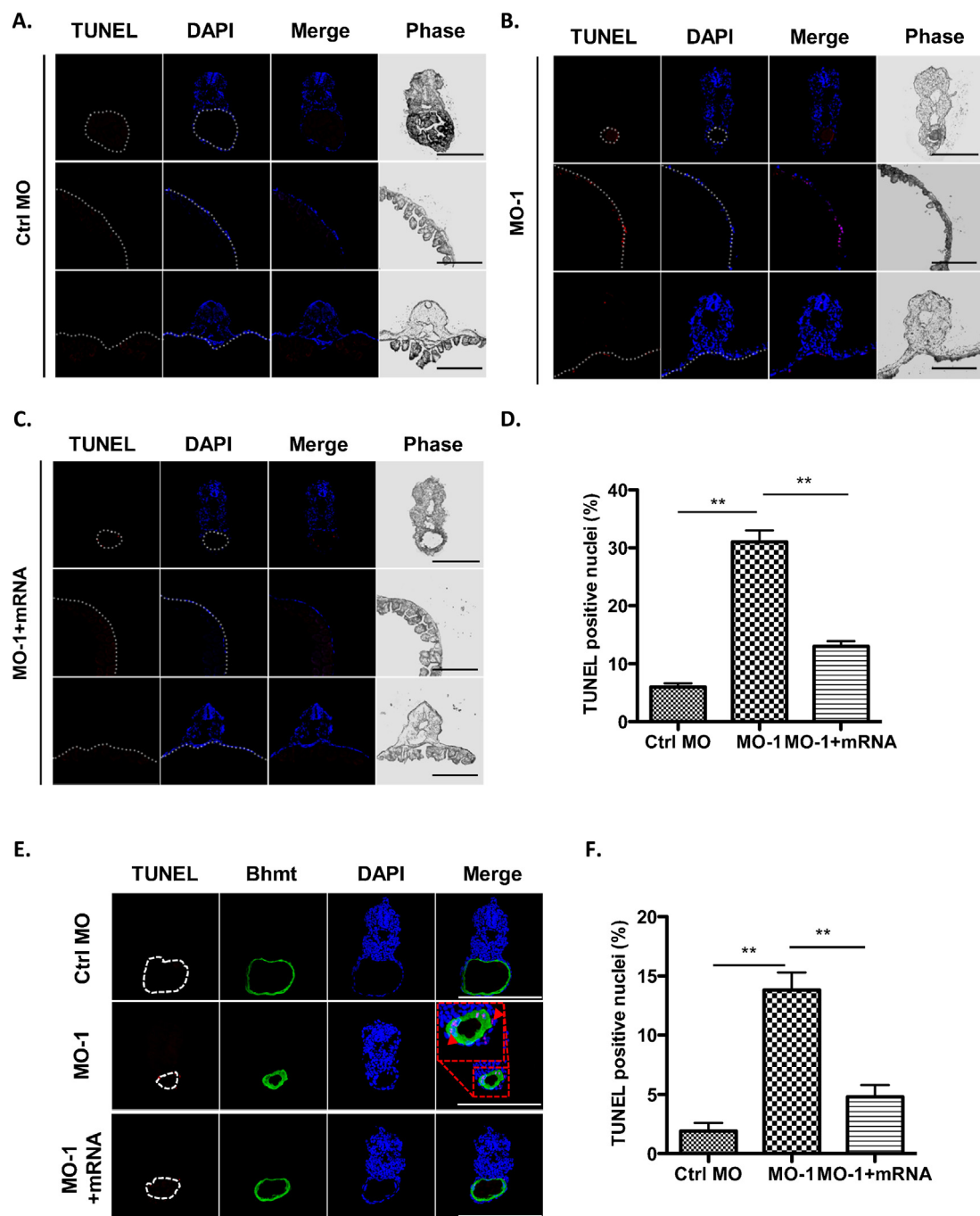


**Fig. 4.** Yolk extension defects in *Rnasel5* morphants is resulted from increased DNA damage at the YSL and the external tissue layers. (A–C) TUNEL assay was performed on the cryosections of morphants with TRITC labeled positive cells and DAPI-labeled nuclei, scale bar 100 μm. The dot lines indicate the overlying layers of yolk. The upper panel is the cross sections of the middle trunk including yolk extension, the middle and down panels is cross sections of the front trunk including yolk ball. (D) Quantitative analysis data of TUNEL positive nuclei. (E) TUNEL and Bhmt staining double assay shows DNA damage are most in YSL as well as external tissue layers of yolk. The red arrow show TUNEL positive staining nuclei in external tissue layers, scale bar 100 μm. (F) Quantitative analysis data of TUNEL positive nuclei. All differences are significant, \*\*: P<0.01. (For interpretation of the references to color in this figure legend, the reader is referred to the web version of the article.)

course, a tissue specific *Rnasel5* knock out fish would more than be necessary to further confirm this phenotype.

It is notable that morpholinos are widely used as a tool for gene silencing, but may have off-target effects mediated by p53 activation (Ekker and Larson, 2001), usually resulting in smaller eyes and heads, abnormal notochord and somite, as well as significant neural death at the end of segmentation (1 dpf) (Gerety and Wilkinson, 2011). The key way to distinguish a morpholino's phenotype from off-target effects is to rescue it with mRNA construct of the respective gene in morphants (Robu et al., 2007). Here, we rescued the

morphological defects in *Rnasel5* morphants by co-injection of full-length *Rnasel5* mRNA. Besides, we used two different MOs targeting distinct sites and detected none apoptotic cells in neural system in *Rnasel5* morphants at 24 hpf by TUNEL assay (Fig. 4).

Consistently, it has been reported that RNASE5, the human homologue of *Rnasel5*, can interact with p53 to inhibit its phosphorylation, which in turn increases p53-Mdm2 interaction, and consequently enhances p53 degradation (Sadagopan et al., 2012). RNASE5 can also inhibit both mitochondria and death receptor apoptotic pathways to prevent stress-induced apoptosis (Li et al.,

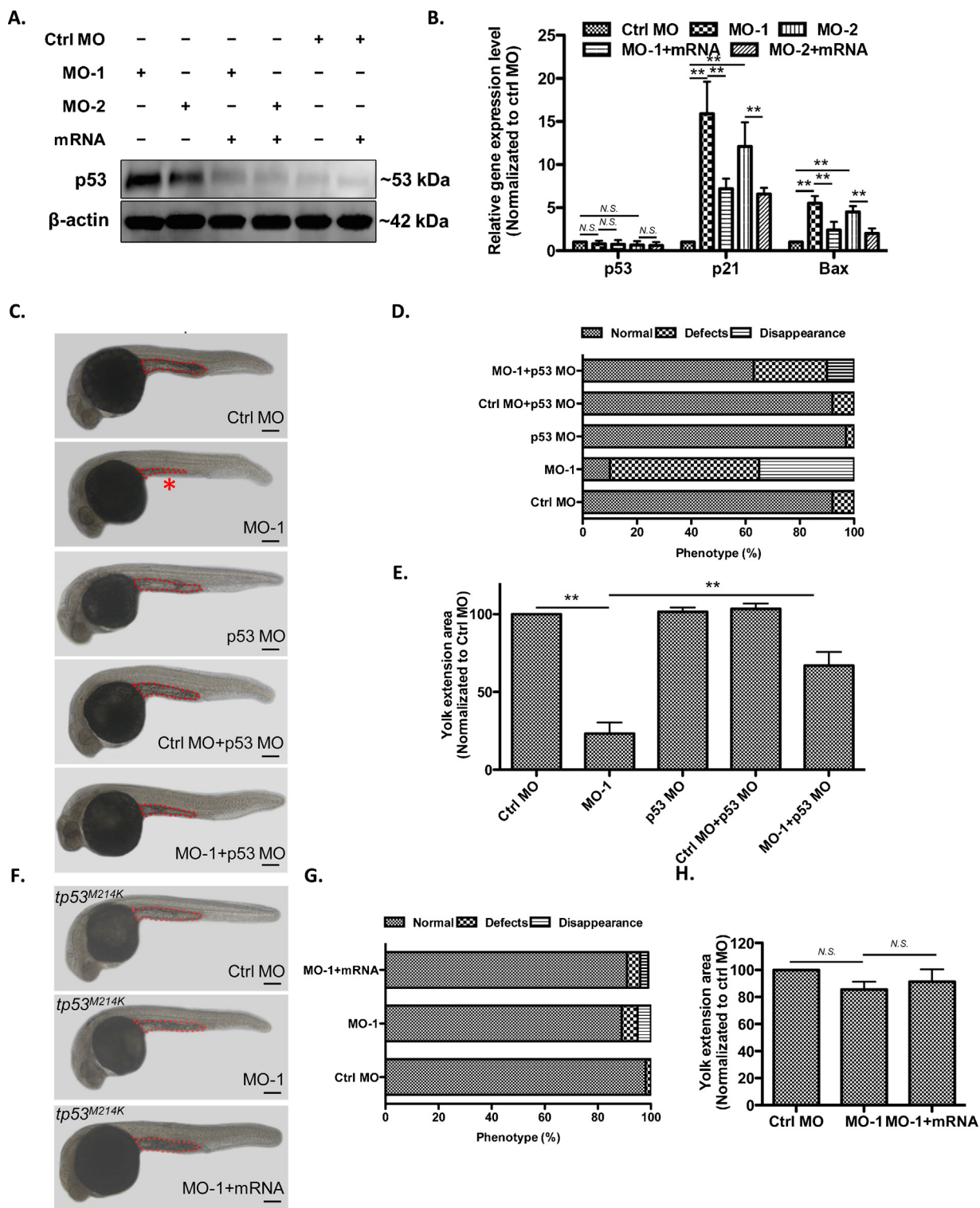


**Fig. 5.** p53 pathway is activated in *Rnasel5* morphants and is associated with yolk extension defects. (A) Western blot analysis of p53 protein expression level under different treatments as indicated. (B) RT-qPCR assays of mRNA level of p53 and p53 and its target genes *p21* and *Bax*. (C) Photographs of 24 hpf embryos under different treatments as indicated. The shrunken yolk extension was identified with asterisk, scale bar 100 μm. (D) Quantitative data of different morphological phenotype in each group as indicated. (E) The relative yolk extension area of different groups as indicated. (F) Yolk extension phenotype in *tp53M214K* transgenic fish line under different treatment, and the quantitative analysis data were analyzed in (G) and (H), scale bar 100 μm.

2010, 2012). In our *Rnasel5* morphants, p53 protein was significantly up-regulated; however, its mRNA remained unchanged (Fig. 5B), strongly suggesting that *Rnasel5* may promote the ubiquitination of zebrafish p53 and enhance its degradation through the same pathway instigated by human RNASE5. Our results, on

other hand, reflect that zebrafish *Rnasel5* is a good representative for the study of human RNASE5 in development. Taken together, our data suggest that *Rnasel5* is essential for the development of yolk extension through repressing the activation of p53.

## Acknowledgments

We thank Professor Jinrong Peng (Zhejiang University College of Animal Sciences) for discussions and supports on the study. We thank Core Facilities at Zhejiang University School of Medicine for the technical assistance. We also thank Chi Luo (Dana-Farber Cancer Institute/Harvard Medical School) for critical reading of the manuscript. This work was supported by National Natural Science Foundation of China grants nos. 81372303 and 31170721 (to Zhengping Xu).

## References

- Chakraborty, A., Uechi, T., Higa, S., Torihara, H., Kenmochi, N., 2009. Loss of ribosomal protein L11 affects zebrafish embryonic development through a p53-dependent apoptotic response. *PLoS One* 4, e4152.
- Chen, G.D., Chou, C.M., Hwang, S.P., Wang, F.F., Chen, Y.C., Hung, C.C., et al., 2006. Requirement of nuclear localization and transcriptional activity of p53 for its targeting to the yolk syncytial layer (YSL) nuclei in zebrafish embryo and its use for apoptosis assay. *Biochem. Biophys. Res. Commun.* 344, 272–282.
- Chen, J., Ng, S.M., Chang, C., Zhang, Z., Bourdon, J.C., Lane, D.P., et al., 2009. p53 isoform delta113p53 is a p53 target gene that antagonizes p53 apoptotic activity via BclXL activation in zebrafish. *Genes Dev.* 23, 278–290.
- Crow, K.D., Amemiya, C.T., Roth, J., Wagner, G.P., 2009. Hypermutability of HoxA13A and functional divergence from its paralog are associated with the origin of a novel developmental feature in zebrafish and related taxa (Cypriniformes). *Evolution Int. J. Org. Evolution* 63, 1574–1592.
- Davidson, A.J., Ernst, P., Wang, Y., Dekens, M.P., Kingsley, P.D., Palis, J., et al., 2003. cdx4 mutants fail to specify blood progenitors and can be rescued by multiple hox genes. *Nature* 425, 300–306.
- Ekker, S.C., Larson, J.D., 2001. Morphant technology in model developmental systems. *Genesis* 30, 89–93.
- Gao, X., Xu, Z., 2008. Mechanisms of action of angiogenin. *Acta Biochim. Biophys. Sin.* 40, 619–624.
- Gerety, S.S., Wilkinson, D.G., 2011. Morpholino artifacts provide pitfalls and reveal a novel role for pro-apoptotic genes in hindbrain boundary development. *Dev. Biol.* 350, 279–289.
- Isken, A., Holzschuh, J., Lampert, J.M., Fischer, L., Oberhauser, V., Palczewski, K., et al., 2007. Sequestration of retinyl esters is essential for retinoid signaling in the zebrafish embryo. *J. Biol. Chem.* 282, 1144–1151.
- Kazakou, K., Holloway, D.E., Prior, S.H., Subramanian, V., Acharya, K.R., Ribonuclease, 2008. A homologues of the zebrafish: polymorphism, crystal structures of two representatives and their evolutionary implications. *J. Mol. Biol.* 380, 206–222.
- Li, Z., Korzh, V., Gong, Z., 2007. Localized rbp4 expression in the yolk syncytial layer plays a role in yolk cell extension and early liver development. *BMC Dev. Biol.* 7, 117.
- Li, S., Yu, W., Kishikawa, H., Hu, G.F., 2010. Angiogenin prevents serum withdrawal-induced apoptosis of P19 embryonal carcinoma cells. *FEBS J.* 277, 3575–3587.
- Li, S., Yu, W., Hu, G.F., 2012. Angiogenin inhibits nuclear translocation of apoptosis inducing factor in a Bcl-2-dependent manner. *J. Cell. Physiol.* 227, 1639–1644.
- Lyman Gingerich, J., Lindeman, R., Putiri, E., Stolzmann, K., Pelegri, F., 2006. Analysis of axis induction mutant embryos reveals morphogenetic events associated with zebrafish yolk extension formation. *Dev. Dyn.* 235, 2749–2760.
- Mizuno, T., Yamaha, E., Kuroiwa, A., Takeda, H., 1999. Removal of vegetal yolk causes dorsal deficiencies and impairs dorsal-inducing ability of the yolk cell in zebrafish. *Mech. Dev.* 81, 51–63.
- Monti, D.M., Yu, W., Pizzo, E., Shima, K., Hu, M.G., Di Malta, C., et al., 2009. Characterization of the angiogenic activity of zebrafish ribonucleases. *FEBS J.* 276, 4077–4090.
- Ober, E.A., Schulte-Merker, S., 1999. Signals from the yolk cell induce mesoderm, neuroectoderm, the trunk organizer, and the notochord in zebrafish. *Dev. Biol.* 215, 167–181.
- Pizzo, E., Buonanno, P., Di Maro, A., Ponticelli, S., De Falco, S., Quarto, N., et al., 2006. Ribonucleases and angiogenins from fish. *J. Biol. Chem.* 281, 27454–27460.
- Pizzo, E., Merlini, A., Turano, M., Russo Krauss, I., Coscia, F., Zanfardino, A., et al., 2011. A new RNase sheds light on the RNase/angiogenin subfamily from zebrafish. *Biochem. J.* 433, 345–355.
- Quarto, N., Pizzo, E., D'Alessio, G., 2008. Temporal and spatial expression of RNases from zebrafish (*Danio rerio*). *Gene* 427, 32–41.
- Robu, M.E., Larson, J.D., Nasevicius, A., Beiraghi, S., Brenner, C., Farber, S.A., et al., 2007. p53 activation by knockdown technologies. *PLoS Genet.* 3, e78.
- Sadagopan, S., Veettil, M.V., Chakraborty, S., Sharma-Walia, N., Paudel, N., Bottero, V., et al., 2012. Angiogenin functionally interacts with p53 and regulates p53-mediated apoptosis and cell survival. *Oncogene* 31, 4835–4847.
- Sheng, J., Luo, C., Jiang, Y., Hinds, P.W., Xu, Z., Hu, G.F., 2014. Transcription of angiogenin and ribonuclease 4 is regulated by RNA polymerase III elements and a CCCTC binding factor (CTCF)-dependent intragenic chromatin loop. *J. Biol. Chem.* 289, 12520–12534.
- Virta, V.C., Cooper, M.S., 2011. Structural components and morphogenetic mechanics of the zebrafish yolk extension, a developmental module. *J. Exp. Zoolog. Part B Mol. Dev. Evol.* 316, 76–92.
- Yang, S.L., Aw, S.S., Chang, C., Korzh, S., Korzh, V., Peng, J., 2011. Depletion of Bhmt elevates sonic hedgehog transcript level and increases beta-cell number in zebrafish. *Endocrinology* 152, 4706–4717.